

Measurement of the Flux of Ultrahigh Energy Cosmic Rays from Monocular Observations by the High Resolution Fly's Eye Experiment.

T. Abu-Zayyad,¹ G. Archbold,¹ J.A. Bellido,² K. Belov,¹ J.W. Belz,³ D.R. Bergman,⁴ J. Boyer,⁵ Z. Cao,¹ R.W. Clay,² B.R. Dawson,² A.A. Everett,¹ J.H.V. Girard,¹ R.C. Gray,¹ W.F. Hanlon,⁴ B.F. Jones,¹ C.C.H. Jui,¹ D.B. Kieda,¹ K. Kim,¹ B. Knapp,⁵ E.C. Loh,¹ K. Martens,¹ G. Martin,⁶ N. Manago,⁷ E.J. Mannel,⁵ J.A.J. Matthews,⁶ J.N. Matthews,¹ J.R. Meyer,¹ S.A. Moore,¹ P. Morrison,¹ A.N. Moosman,¹ J.R. Mumford,¹ M.W. Munro,³ L. Perera,⁴ K. Reil,¹ M. Roberts,⁶ M. Sasaki,⁷ M. Seman,⁵ M.A. Schindel,³ S. Schnetzer,⁴ P. Shen,¹ K.M. Simpson,² J.D. Smith,¹ P. Sokolsky,¹ C. Song,⁵ R.W. Springer,¹ B.T. Stokes,¹ S.B. Thomas,¹ G.B. Thomson,⁴ S. Westerhoff,⁵ L.R. Wiencke,¹ T.D. VanderVeen,¹ A. Zech,⁴ and X. Zhang⁵

(The High Resolution Fly's Eye Collaboration)

¹University of Utah, Department of Physics and High Energy Astrophysics Institute, Salt Lake City, Utah, USA

²University of Adelaide, Department of Physics, Adelaide, South Australia, Australia

³University of Montana, Department of Physics and Astronomy, Missoula, Montana, USA.

⁴Rutgers University — The State University of New Jersey,

Department of Physics and Astronomy, Piscataway, New Jersey, USA

⁵Columbia University, Department of Physics and Nevis Laboratory, New York, New York, USA

⁶University of New Mexico, Department of Physics and Astronomy, Albuquerque, New Mexico, USA

⁷University of Tokyo, Institute for Cosmic Ray Research, Kashiwa, Japan

We have measured the cosmic ray spectrum above 10^{17} eV using the two air fluorescence detectors of the High Resolution Fly's Eye observatory operating in monocular mode. We describe the detector, photo-tube and atmospheric calibrations, and the analysis techniques for the two detectors. We fit the spectrum to a model consisting of galactic and extra-galactic sources. The measured spectrum is consistent with this two-component model including the GZK cutoff.

The highest energy cosmic rays detected so far, of energies up to and above 10^{20} eV, are very interesting in that they shed light on two important questions: the nature of their origin in astrophysical or other sources and their propagation to us through the Cosmic Microwave Background Radiation (CMBR). The production of pions from interactions of CMBR photons and Ultra High Energy (UHE) cosmic rays is an important energy loss mechanism above about 6×10^{19} eV, and is called the Greisen-Zatsepin-K'uzmin (GZK) cut-off [1, 2]; e^+e^- production in the same collisions is a somewhat weaker energy-loss mechanism above a threshold of about 7×10^{17} eV. We report here a measurement of the flux of UHE cosmic rays from 2×10^{17} eV to over 10^{20} eV with the High Resolution Fly's Eye (HiRes) observatory.

The HiRes observatory consists of two air-fluorescence detector sites separated by 12.6 km and located at the U.S. Army Dugway Proving Ground in Utah. Cosmic rays interacting in the upper atmosphere initiate particle cascades known as extensive air-showers. Passage of charged particles excites nitrogen molecules causing emission of ultraviolet light. The HiRes experiment was designed to detect this fluorescence light stereoscopically. The fluorescence yield per particle has been previously measured [3]. From the observed signal and its longitudinal development, we can infer the arrival direction, energy, and composition of the primary cosmic ray. In this paper we present the cosmic ray energy spectra, measured in monocular mode, from the two detectors.

The two HiRes detector sites, referred to as HiRes-

I and HiRes-II, are operated on clear, moon-less nights. Over a typical year, each detector accumulates up to 1000 hours of observation. The HiRes-I site has been in operation since June of 1997 [4]. It consists of 22 detector units, each equipped with a 5 m^2 spherical mirror and 256 photo-tube pixels at its focal plane. Each photo-tube covers a 1° cone of sky. Together, the 22 mirrors provide nearly full azimuthal coverage for elevation angles between 3° and 17° . The HiRes-I detectors perform sample-and-hold integration in a $5.6 \mu\text{s}$ time window, which is long enough to contain signals from all reconstructible events. The HiRes-II site was completed in late 1999 and began observations that year. This site uses the same mirrors and photo-tubes as HiRes-I, but contains 42 mirrors, in two rings, covering elevation angles from 3° to 31° . HiRes-II uses an FADC data acquisition system operating at 10 MHz [5].

To determine the correct shower energies, the air fluorescence technique requires accurate measurement and monitoring of photo-tube gains. Two methods of calibration are in use. Pulses from a YAG laser are distributed to mirrors via optical fibers. They provide a nightly relative calibration. A stable, standard light source is used for a more precise monthly absolute calibration. Overall, the relative photo-tube gains were stable to within 3.5% and the absolute gains were known to within $\pm 10\%$ [6].

A second variable in energy measurement is atmospheric clarity. Light from air showers is attenuated by: (a) molecular (Rayleigh), and (b) aerosol scattering. The former is approximately constant, subject only to small

variations in the atmospheric overburden. The aerosol concentration needs to be monitored continually. HiRes measures the aerosol content by observing scattered light from two steerable laser systems. The lasers observed by HiRes-I has been in operation since 1999. The vertical aerosol optical depth from ground to 3.5 km altitude, τ_A , is measured each hour. These measurements yielded an average τ_A at 355 nm of 0.04 [7]. The RMS of the distribution is 0.02, and the systematic uncertainty in the mean is less than this. The average aerosol ground-level horizontal extinction length, Λ_H was determined to be 25 km. Therefore, our analysis used an exponential aerosol density profile with a scale height of $H_A = 1.0$ km and $\Lambda_H = 25.0$ km, corresponding to an average optical depths, $\tau_A = H_A/\Lambda_H = 0.04$.

Between June 1997 and September 2001, the HiRes-I detector operated for approximately 3100 hours. From this, 2410 hours of good weather data were selected. This data set contained 125 million triggers, mostly noise events. A subset of 4.7 million downward track-like events were found. For these events, a shower-detector plane was determined from the pattern of photo-tube hits. We then excluded events containing an average number of photo-electrons per photo-tube of less than 25; for these the fluctuations in signals are too great to permit reliable reconstruction of the shower profile. Lastly, we cut out tracks with angular speed in excess of $3.33^\circ/\mu\text{s}$, which are typically within 5 km of HiRes-I. For these events, the shower maxima appear above the field of view. We selected 10,968 events for reconstruction.

Determination of the shower geometry is possible using a single detector (i.e. in monocular mode) by fitting the photo-tube trigger times, t_i , to the following function of their viewing angles, χ_i , measured in the event plane from the horizontal [8]:

$$t_i = t_0 + \frac{R_p}{c} \tan\left(\frac{\pi - \psi - \chi_i}{2}\right). \quad (1)$$

Here R_p is the impact parameter, ψ the in-plane angle between the shower and the horizontal plane containing the detector, and t_0 the time of closest approach. With limited elevation coverage, HiRes-I monocular events are too short in angular spread for reliable determination of ψ and R_p by timing alone. For this analysis, the expected form of the shower development itself was used to constrain the time fit to yield realistic geometries. The shower profile was assumed to be described by the Gaisser-Hillas parameterization [9]

$$N(x) = N_m \left(\frac{x - x_0}{x_m - x_0} \right)^{(x_m - x_0)/\lambda} \exp\left(\frac{x_m - x}{\lambda}\right), \quad (2)$$

where $N(x)$, N_m are the number of particles at depth x and at shower maximum depth, x_m , respectively. The first-interaction depth and shower elongation constant

are denoted by x_0 and λ . This technique is called the Profile-Constrained Fit (PCF).

Equation 2 is in good agreement with previous HiRes measurements [10] and with CORSIKA/QGSJET simulations [11, 12, 13]. We fixed x_0 and λ at 40 and 70 g/cm^2 , respectively. We allowed x_m to vary in 35 g/cm^2 steps between 680 and 900 g/cm^2 , matching the expected range of x_m for proton to iron primaries in this energy range. Next, cuts were made to require a minimum track arc length of 8.0° and a maximum depth for the highest elevation hit photo-tube of 1000 g/cm^2 . Significant contamination from direct Čerenkov light degrades the reliability of the PCF. Therefore, we also rejected tracks with $\psi > 120^\circ$ and those with two or more bins with $>25\%$ Čerenkov light. A total of 5,264 events remained after processing.

Monte Carlo (MC) studies were performed to assess the reliability of the PCF method. The simulated events were subjected to the same selection criteria and cuts imposed on the data. Not including atmospheric fluctuations, an RMS energy resolution of better than 20% was seen above $3 \times 10^{19} \text{ eV}$. However, the resolution degrades at lower energies to about 25% at $3 \times 10^{18} \text{ eV}$. These MC results were cross-checked by examination of a small set of stereo events where the geometry is more precisely known. Comparing the energies reconstructed using monocular and stereo geometries, we obtained energy resolutions similar to those seen in the MC.

The MC simulation is also used to calculate the detector aperture. Here the simulated events were subjected to the same reconstruction algorithm and cuts applied to the data. To verify the reliability of this calculation, we compared, at different energies, the zenith angle (θ) and impact parameter (R_p) distributions, which define the detector aperture. The MC predictions for these are very sensitive to details of the simulation, including the detector triggering, optical ray-tracing, signal/noise, and the atmospheric modeling. We saw excellent agreement between data and MC. For example, we show the comparison of R_p distributions at three energies in Figure 1.

The analysis of HiRes-II monocular data was similar to that for HiRes-I. The data sample was collected during 142 hours of good weather between Dec. 1999 and May 2000. With the greater elevation coverage at HiRes-II, it was feasible to reconstruct the shower geometry from timing alone (the PCF is unnecessary), therefore we were able to loosen some cuts for the HiRes-II fits. Since Eqn. 1 is linear in R_p and t_0 , we find the best value for these variables analytically for each ψ ; the best ψ is then found by χ^2 minimization. At this stage 104,048 downward (in elevation angle) events remained.

With the geometry of the shower known, we fit the observed light signal to the Gaisser-Hillas parameterization (Eqn. 2). We collected photo-electrons from all tubes into a sequence of time bins. This exploited the FADC data acquisition system and lessened our sensitivity to photo-

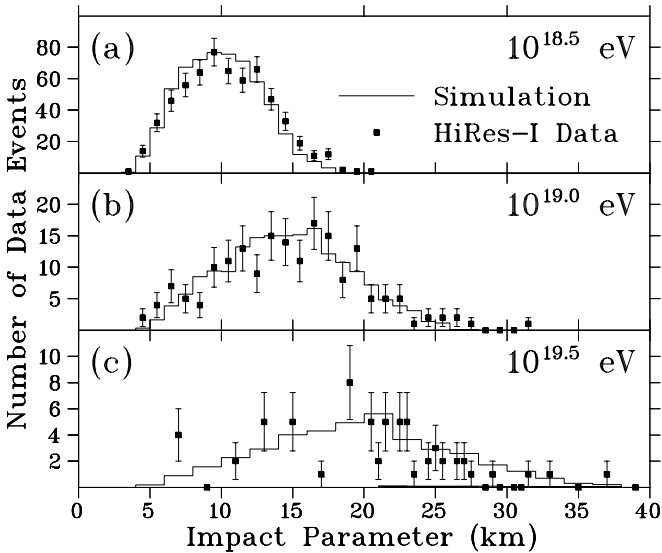


FIG. 1: Comparison of HiRes-I simulated (histogram) and observed (points) R_p distributions at (a) $10^{18.5}$, (b) $10^{19.0}$, and (c) $10^{19.5}$ eV. The MC distributions are normalized to the number of data events.

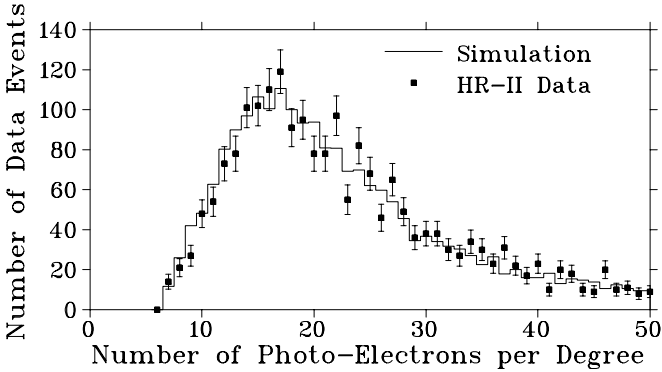


FIG. 2: A comparison of the number of photo-electrons per degree of track seen in HiRes-II monocular events (data points) and in simulation (histogram).

tube acceptance. The events were required to have a good fit to the Gaisser-Hillas function. They were also required to have a track length greater than 10° for upper ring or multi-mirror events, a track length greater than 7° for lower ring events, an angular speed less than $11^\circ/\mu\text{s}$, a zenith angle less than 60° , and a shower maximum visible in our detector. There was also a cut on the size of the Čerenkov light subtraction at $< 60\%$ of signal. Again, the same selections and cuts were applied to both simulated and real events. The PCF technique used by the HiRes-I analysis required tighter cuts than is made here for the HiRes-II pure timing fits. There were 781 events left after these cuts. We also found the simulations gave an excellent reproduction of the data, as seen, for example, in the comparison of the number of photo-electrons per degree of track in Fig. 2.

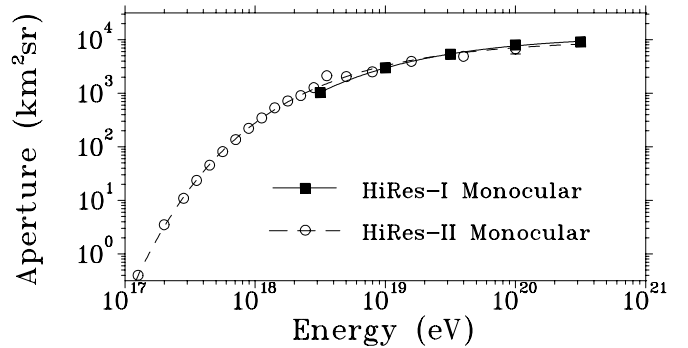


FIG. 3: Calculated HiRes monocular Reconstruction aperture in the energy range 10^{17} – 3×10^{20} eV. The HiRes-I and -II apertures are shown by the squares and circles, respectively.

For both HiRes-I and HiRes-II events, the photo-electron count was converted to a shower size at each atmospheric depth, using the known geometry of the shower, and corrected for atmospheric attenuation. We integrated the resulting function over x (using the determined values of N_m and x_m) and then multiplied by the average energy loss per particle to give the visible shower energy. A correction for energy carried off by non-observable particles to give the total shower energy ($\sim 10\%$) [11] was then applied.

The monocular reconstruction apertures are shown in Fig. 3; both HiRes-I and HiRes-II approach $10^4 \text{ km}^2 \text{ steradian}$ above 10^{20} eV. We restrict our result for HiRes-I to energies $> 3 \times 10^{18}$ eV; below this energy the PCF technique is unstable. Due to longer tracks and additional timing information, the RMS energy resolution for HiRes-II remains better than 30% down to 10^{17} eV. However, the HiRes-II data sample becomes statistically depleted above 10^{19} eV.

We calculated the cosmic ray flux for HiRes-I above 3×10^{18} eV, and for HiRes-II above 2×10^{17} eV. This combined spectrum is shown in Fig. 4, where the flux $J(E)$ has been multiplied by E^3 . The error bars represent the 68% confidence interval for the Poisson fluctuations in the number of events only. The HiRes-I flux is the result of two completely independent analyses [14, 15], which yielded essentially identical flux values.

The largest systematic uncertainties are the absolute calibration of the photo-tubes ($\pm 10\%$) [6], the yield of the fluorescence process ($\pm 10\%$) [3], the correction for unobserved energy in the shower ($\pm 5\%$) [11, 16], and the modeling of the atmosphere [7]. To test the sensitivity of the flux measurement to atmospheric uncertainties, we generated new MC samples with τ_A altered by ± 1 RMS value, from 0.04 to 0.06 and 0.02, respectively. The data and new MC samples were then reconstructed with the altered atmospheric parameters. Averaged over energy, the flux $J(E)$ changed symmetrically by a corresponding ($\pm 15 \pm 5\%$). The systematic uncertainty in the mean τ_A value is smaller than the RMS deviation of 0.02. This

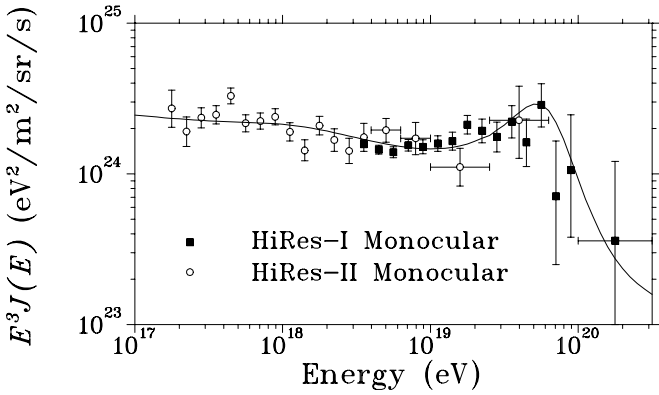


FIG. 4: Combined HiRes monocular energy spectrum. The squares and circles represent the cosmic ray differential flux $J(E)$, multiplied by E^3 , measured by HiRes-I and HiRes-II, respectively. The line is a fit to the data of a model, described in the text, of galactic and extra-galactic cosmic ray sources.

$\pm 15\%$ change therefore represents a conservative overestimate of the one standard deviation systematic uncertainty from atmospheric effects. If we add in quadrature this uncertainty to the others mentioned above, we find a net systematic uncertainty in $J(E)$ of 21%. This uncertainty is common to the fluxes for HiRes-I and HiRes-II. There is an additional relative calibration uncertainty between the two sites which is less than 10%.

Our spectrum contains five events above the GZK cutoff at 6×10^{19} eV [1, 2], and one above 10^{20} eV. The reconstructed energy of the highest event in this sample is 1.8×10^{20} eV. The fitted geometry was insensitive to variations in aerosol parameters. Assuming a purely molecular atmosphere ($\tau_A = 0.0$), we obtain a lower energy limit of 1.5×10^{20} eV.

In the energy range where both detectors' data have good statistical power the results agree with each other very well. The data are consistent with previous experiments which observed the second knee at about 7×10^{17} eV, and the ankle at about 4×10^{18} eV [17].

Our data from $\log E$ of 18.7 to 19.8 shows an $E^{-2.8}$ power law behavior. But our three data points above 19.8 are not consistent with that power law continuing (19.1 events are predicted where only 4 are observed, a Poisson probability of 1.4×10^{-4}). Our data are consistent with the GZK cutoff. As an example of what one would expect, we have fit the data to a model that consists of galactic and extra-galactic sources, that includes the GZK cutoff. We use the extra-galactic source model of Berezhinsky *et al.* [18] which assumes that protons come from sources distributed uniformly across the universe, with a maximum energy at the source of 10^{21} eV, and that they lose energy by pion and e^+e^- production from

the CMBR, as well as from the expansion of the universe. Since the measured composition [17] is heavy at the lower end of our energy range, with an iron content decreasing linearly with $\log E$, we approximate the galactic component of cosmic rays as falling with an $E^{-3} \times (19.5 - \log E)$ spectrum between $17.0 < \log E(\text{eV}) < 19.5$. The fitting parameters of the model are the normalization of the galactic flux, the power law index, and normalization (at the source) of extra-galactic cosmic rays. The model prediction includes the experimental resolution. The fit is good with χ^2 of 40.5 for 32 degrees of freedom. In this model the peak at $\log E$ of 19.8 is due to pion production pile-up, the ankle is made by losses due to e^+e^- production, and the second knee comes from e^+e^- production pile-up.

This work is supported by US NSF grants PHY-9322298, PHY-9321949, PHY-9974537, PHY-9904048, PHY-0071069, by the DOE grant FG03-92ER40732, and by the Australian Research Council. We gratefully acknowledge the contributions from the technical staffs of our home institutions. The cooperation of Colonel E. Fischer, the US Army, and the Dugway Proving Ground staff is greatly appreciated.

- [1] K. Greisen, Phys. Rev. Lett. **16**, 748, (1966).
- [2] G.T. Zatsepin and V.A. K'uzmin, Pis'ma Zh. Eksp. Teor. Fiz. **4**, 114 (166) [JETP Lett. **4**, 78 (1966)].
- [3] F. Kakimoto *et al.*, NIM **A 372**, 527 (1996).
- [4] T. Abu-Zayyad *et al.*, Proc. 26th Int. Cosmic Ray Conf. (Salt Lake City), **5**, 349, (1999).
- [5] J. Boyer, B. Knapp, E. Mannel, and M. Seman, NIM **A482**, 457 (2002).
- [6] T. Abu-Zayyad *et al.*, to be submitted to NIM.
- [7] T. Abu-Zayyad *et al.*, in preparation.
- [8] R.M. Baltrusaitis *et al.*, NIM **A240**, 410 (1985).
- [9] T. Gaisser and A.M. Hillas, Proc. 15th Int. Cosmic Ray Conf. (Plovdiv), **8**, 353, (1977).
- [10] T. Abu-Zayyad *et al.*, Astropart. Phys. **16**, 1, (2001).
- [11] C. Song, Z. Cao *et al.*, Astropart. Phys. **14**, 7, (2000).
- [12] D. Heck, J. Knapp, J.N. Capdevielle, G. Schatz and T. Thouw "CORSIKA : A Monte Carlo Code to Simulate Extensive Air Showers", Report FZKA 6019 (1998), Forschungszentrum Karlsruhe.
- [13] N.N. Kalmykov, S.S. Ostapchenko and A.I. Pavlov, Nucl. Phys. B (Proc. Suppl.) **52B**, 17, (1997).
- [14] T. Abu-Zayyad, Ph.D Thesis, University of Utah (2000).
- [15] X. Zhang, Ph.D Thesis, Columbia University (2001).
- [16] J. Linsley, Proc. 18th Int. Cosmic Ray Conf. (Bangalore), **12**, 135, (1983).
- [17] D.J. Bird *et al.*, Phys. Rev. Lett. **71**, 3401, (1993).
- [18] V. Berezhinsky, A.Z. Gazizov, and S.I. Grigorieva, hep-ph/0204357.